OCEANS AND ATMOSPHERE
www.csiro.au

The aerial survey index of abundance: updated results for the 2013/14 fishing season

Paige Eveson, Jessica Farley and Mark Bravington

CCSBT-ESC/1409/18

Prepared for the CCSBT Extended Scientific Committee for the 19th Meeting of the Scientific Committee, 1-6 September 2014, Auckland, New Zealand

CSIRO Oceans and Atmosphere Flagship

Citation

Eveson P, Farley J, Bravington M (2014). The aerial survey index of abundance: updated results for the 2013/14 fishing season. CCSBT-ESC/1409/18, 19th Meeting of the Scientific Committee, 1-6 September 2014, Auckland, New Zealand.

Copyright and disclaimer

Important disclaimer

Acknowledgments

There are many people we would like to recognise for their help and support during this project. We would especially like to thank this year's observers (spotters), pilots and data recorders; Darren Tressider, Derek Hayman, Andrew Merwood, Mattew Grant, Matthew Lucchesi, John Veerhius, Thor Carter and Jim Dell. We also appreciate the support given to us by the commercial tuna spotters and pilots during the survey especially for providing information on weather condition during flights. This study was funded by AFMA, Department of Agriculture, CCSBT members, the Australian SBT Industry, and CSIRO's Oceans and Atmosphere Flagship.

Contents

1 Abstract

The estimate of relative juvenile abundance from the 2014 scientific aerial survey is significantly higher than for any previous survey year. The environmental conditions during the 2014 survey were average for the most part, except that the level of haze was higher than in past years. Because increased haze is unfavourable for making sightings, the raw estimate was adjusted upwards slightly in the standardization process. Also, as for past years where there has only been one spotter per plane, the raw estimate was adjusted upwards in the analysis to account for the fact that one spotter tends to make fewer sightings than two spotters. In the past several years (2009-2013), the percentage of schools that were comprised of small fish (<8 kg; estimated to be 1-year-olds) was unusually high, but that was not the case this year.

2 Introduction

The index of juvenile southern bluefin tuna (SBT) abundance based on a scientific aerial survey in the Great Australian Bight (GAB) is one of the few fishery-independent indices available for monitoring and assessment of the SBT stock. The aerial survey was conducted in the GAB between 1991 and 2000, but was suspended in 2001 due to logistic problems of finding trained, experienced observers (spotters). The suspension also allowed for further data analysis and an evaluation of the effectiveness of the survey. A decision to continue or end the scientific aerial survey could then be made on the merits of the data, in particular the ability to detect changes in abundance.

Analysis of the data was completed in 2003 and it showed that the scientific aerial survey does provide a suitable indicator of SBT abundance in the GAB (Bravington 2003). In the light of serious concerns about the reliability of historic and current catch and CPUE data and weak year classes in the late 1990s and early 2000s, this fishery-independent index was considered even more important (Anon 2008). Thus, in 2005, the full scientific line-transect aerial survey was re-established in the GAB, and this survey has been conducted each year since. New analysis methods were developed and have subsequently been refined. Based on these methods, an index of abundance across all survey years has been constructed.

Up until 2010, all planes that flew in the survey had two spotters – a spotting pilot and a dedicated spotter – each searching his own side of the plane. Due to the retirement of the two spotting pilots involved in recent surveys, and the impossibility to replace them, one of the two planes flying in the 2010 survey and both planes flying in the 2011 to 2013 surveys had only one spotter (along with a non-spotting pilot). Solo spotters need to search both sides of the plane and are likely to miss more sightings than two spotters. In anticipation of this significant change to the survey, calibration experiments were run in parallel with the full scientific aerial survey in 2007-2009 (see Eveson et al. 2007, 2008, 2009 for details). The 2007 experiment served as a pilot study that led to improvements in the design of the 2008 and 2009 experiments. These latter experiments were designed to compare the number of SBT sightings and total estimated biomass of SBT observed by a single spotter in the calibration plane versus two spotters in the survey plane over the same area and time strata. Based on data from these experiments, a method for accounting for the fact that a plane with one observer makes fewer sightings than a plane with two observers was developed in Eveson et al. (2009, 2010) and refined in Eveson et al. (2011). These methods have been applied to the analysis since 2011.

This report summarises the field procedures and data collected during the 2014 season, describes the current methods for analysing the data (which remained the same as in the previous two years), and presents results from applying these methods to the data from all survey years.

3 Methods

3.1 Field procedures

The 2014 aerial survey was conducted in the GAB between 1 January and 31 March. As in previous surveys, two Rockwell Aero Commander 500S were chartered for the season. One aircraft was chartered for the full three months and a second for January and February only. Each plane contained one observer (spotter) and a non-spotting pilot. Both observers used in 2014 were employed in previous seasons; one for the 2005 to 2013 surveys and the other in all surveys.

The aerial survey followed the protocols established for the 2000 survey (Cowling 2000) and used in all subsequent surveys with respect to the area searched, plane flying height and speed, minimum environmental conditions, time of day the survey lines were flown, and data recording protocols. Fifteen north-south transect lines (Figure 1) were surveyed. A complete replicate of the GAB consists of a subset of 12 (of the 15) lines divided into 4 blocks. In the past, the remaining 3 lines in a replicate (either: 1, 3 and 14, or 2, 13 and 15) were not searched, as SBT abundance was historically low in those areas and surveying a subset increases the number of complete replicates of the GAB in the survey. In 2009 and 2011-2013, however, the distribution of SBT in the GAB appears to have changed with an increase in abundance in the eastern GAB compared to the western GAB (see Farley and Basson, 2013). Given this, lines 13, 14 and 15 were not routinely omitted on alternative replicates of the GAB.

When flying along a line, the single observer searched the sea surface for patches of SBT from his side of the plane (the right side) through 180° to the other side of the plane (the left side). When both planes were surveying, they always surveyed neighbouring blocks. The blocks were chosen with the aim of allowing both planes to complete each block at least once per replicate. When conditions allowed for only one plane to survey (e.g. only one block was suitable), then preference was given to the plane with the observer that had not surveyed that block.

The 2014 field operation was successful, largely due to the availability of two planes on days suitable for survey. This year, 7 replicates of the GAB were completed which is similar to 2010-2013, but higher than the 3-5 replicates for the preceding 5 years when only one plane was available for the survey.

Figure 1. Location of the 15 north-south transect lines for the scientific aerial survey in the GAB.

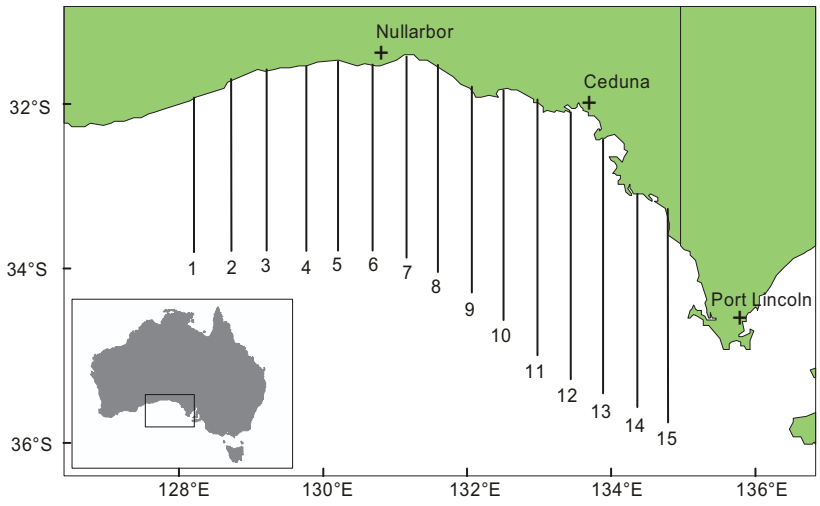

3.2 Data preparation

The data collected from the 2014 survey were loaded into the aerial survey database and checked for any obvious errors or inconsistencies and corrections made as necessary. In order for the analyses to be comparable between all survey years, only data collected in a similar manner from a common area were included in the data summaries and analyses presented in this report. In particular, only search effort and sightings made along north/south transect lines in the unextended (pre-1999) survey area and sightings made within 6 nm of a transect line were included (see Basson et al. 2005 for details). In cases where a sighting consisted of more than one school, then the sighting was included if at least one of the schools was within 6 nm of the line. We excluded secondary sightings and any search distance and sightings made during the aborted section of a transect line (see Eveson et al. 2006 for details).

The data from recent survey years (2009-2013) included an unusually high proportion of schools of small fish estimated to be less than 8kg, which we assume to be the average weight cut-off between 1- and 2-year olds (Table 1). This was first noted in 2011 (Eveson et al. 2011). In the current year, the proportion of schools comprised of such small fish was much lower and similar to values seen in the late 1990s (Table 1). In the CCSBT operating model (OM) and management procedures (MP), the aerial survey index is assumed to provide a relative time series of age 2-4 abundance in the Great Australian Bight. Thus, for consistency with the OM and MP as well as general consistency in interpretation of the index across years, schools estimated to be comprised of 1-year-old fish (i.e., that had an average fish size estimate of less than 8 kg) are omitted from the analysis (see Eveson et al. 2011).

Table 1. Percent of schools in each survey year comprised of fish estimated to be less than 8kg on average (assumed to be 1-year-olds).

YEAR	%	YEAR	%
1993	0.2	2006	0.7
1994	7.4	2007	0.0
1995	8.8	2008	0.7
1996	3.7	2009	13.1
1997	8.2	2010	16.1
1998	6.2	2011	30.7
1999	1.4	2012	25.3
2000	0.8	2013	17.7
2005	2.1	2014	4.1

3.3 Search effort and sightings

A summary of the total search effort and SBT sightings made in each survey year is given in Table 2. All of the values are based on raw data, which have not been corrected for environmental factors or observer effects. This table, and all summary information and results presented in this report, include only the data outlined in the previous section as being appropriate for analysis. Recall that we are omitting schools comprised of fish less than <8 kg on average. Also note that the summary statistics include data from all flights, some of which had only one observer in 2010 and all of which had only one observer in 2011 to 2014 (with the exception of two flights in 2012 and four flights in 2013).

The total distance searched in 2014 was again very high due to the continued (since 2010) availability of two survey planes and reasonably good flying conditions. The raw sightings rate (number of sightings per 100 nm) was above average (Table 2). Similarly, since the sightings were quite large on average (Figure 2), the total biomass per nm was also higher than average, although still not as high as in 2010 and 2011 (Table

2). ***It is important to keep in mind that the statistics for 2010-2014 include data from flights with only one observer, so caution must be used in comparing them directly with previous years for which all flights had two observers because we have shown previously that the sightings rate tends to be lower for flights with only one observer.***

The distribution of sightings was similar to 2013, with most being made in inshore and in the eastern half of the survey area (Figure 3). Note however that there was also a greater percent of sightings along the 6 westernmost lines than since 2006 (Figure 3).

Table 2. Summary of aerial survey data by survey year. Only data considered suitable for analysis (as outlined in text) are included. All biomass statistics are in tonnes. All values in the table are based on raw data, which have not been corrected for environmental factors or observer effects.

SURVEY YEAR	TOTAL DISTANCE SEARCHED (NM)	NUMBER SBT SIGHTINGS	SIGHTINGS PER 100NM	TOTAL BIOMASS	BIOMASS PER NM	AVERAGE PATCHES PER SIGHTING	MAX PATCHES PER SIGHTING	AVERAGE BIOMASS PER PATCH	MAX BIOMASS PER PATCH
1993	7603	129	1.70	12219	1.61	4.0	76	24.5	203
1994	15180	160	1.05	13978	0.92	3.3	23	26.4	247
1995	14573	165	1.13	20149	1.38	3.5	38	34.7	225
1996	12284	110	0.90	16047	1.31	4.0	46	36.5	147
1997	8813	101	1.15	9154	1.04	3.2	18	28.5	203
1998	8550	104	1.22	9764	1.14	2.2	21	42.1	966
1999	7555	50	0.66	2998	0.40	2.5	21	24.2	122
2000	6775	76	1.12	4812	0.71	2.6	17	24.8	100
2005	5968	79	1.32	6043	1.01	2.4	17	32.1	198
2006	5150	43	0.83	4068	0.79	2.0	8	47.9	272
2007	4872	41	0.84	3538	0.73	2.6	11	33.4	123
2008	7462	121	1.62	8009	1.07	3.5	24	19.0	314
2009	8101	145	1.79	7964	0.98	2.5	22	22.3	172
2010[1]	10559	184	1.74	18477	1.75	4.0	41	24.9	539
2011[2]	10148	135	1.33	18559	1.83	2.7	37	50.2	400
2012[2]	10777	48	0.45	4939	0.46	3.2	45	32.1	507
2013[2]	12889	124	0.96	19127	1.48	3.0	18	52.0	634
2014[2]	12238	175	1.43	21213	1.73	2.4	25	49.7	481

[1] Data comes from flights with one observer as well as flights with two observers.
[2] All data comes from flights with one observer (with the exception of one flight in 2012 and 3 flights in 2013).

Figure 2. Frequency of SBT patch sizes (in tonnes) by survey year.

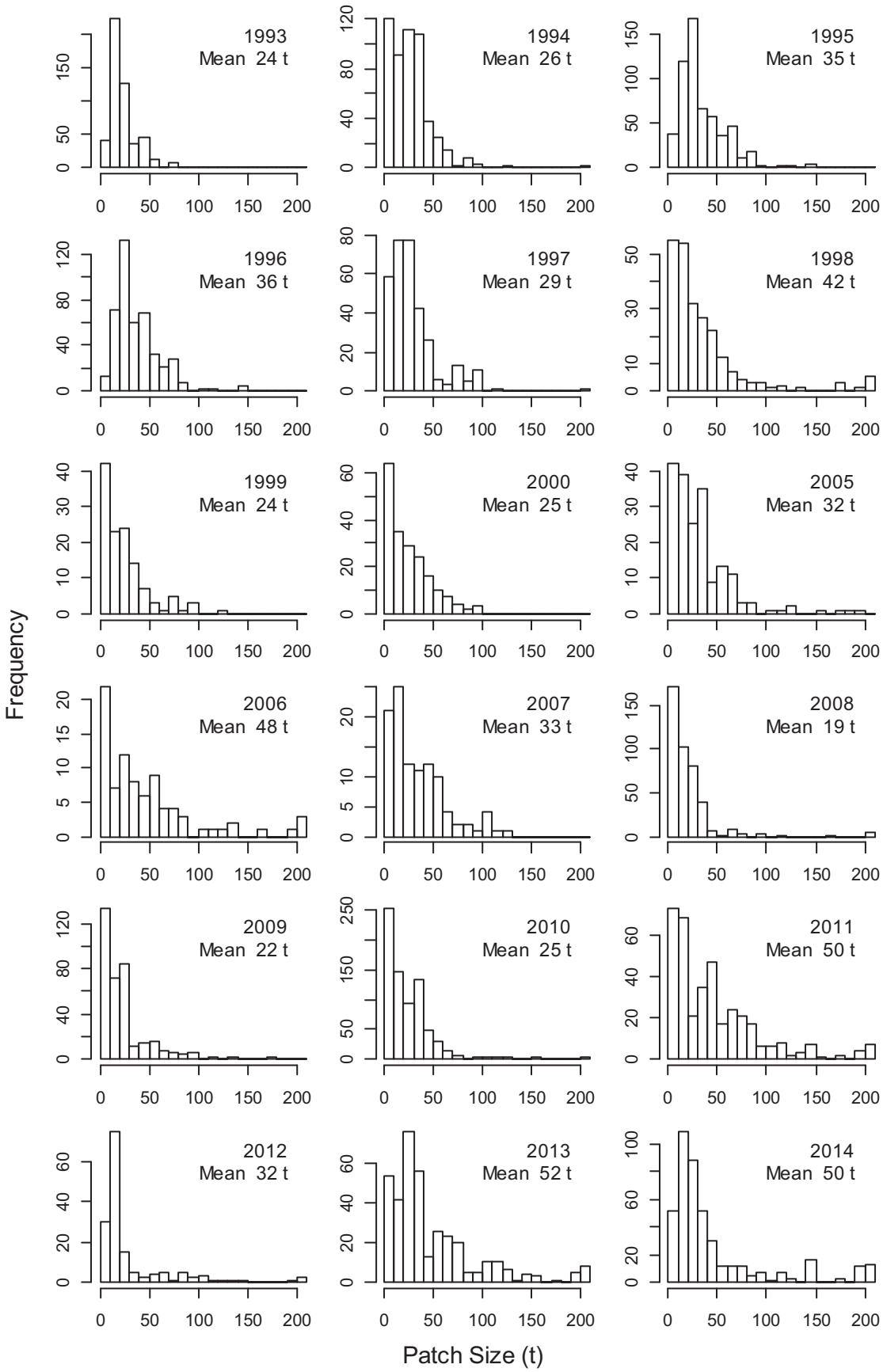

Figure 3. Distribution of SBT sightings made during each aerial survey year. Red circles show the locations of SBT sightings, where the size of the circle is proportional to the size of the sighting, and grey lines show the north/south transect lines that were searched.

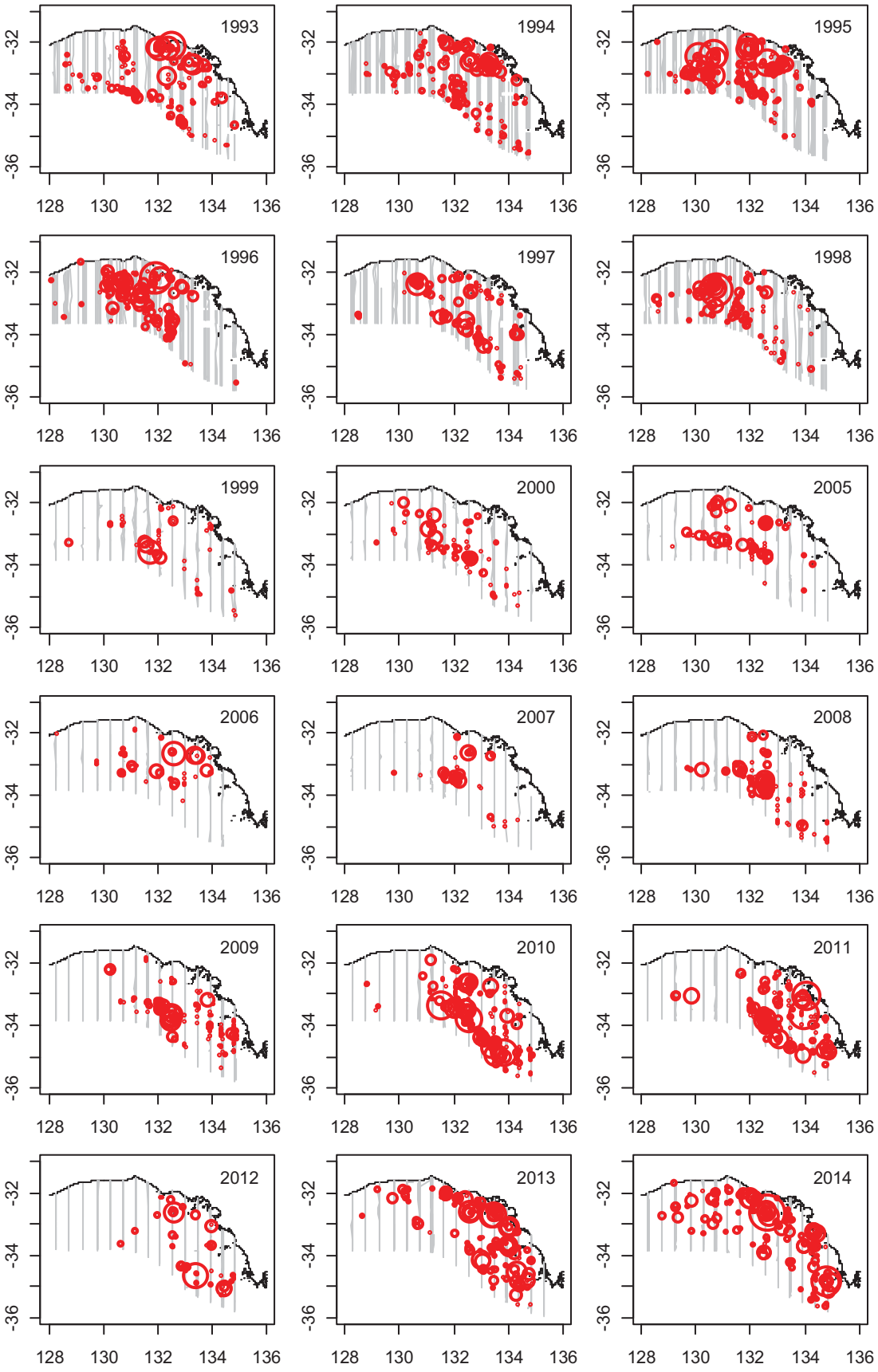

3.4 Environmental variables

Table 3 and Figure 4 summarize the environmental conditions that were present during valid search effort in each survey year. All the environmental variables presented were recorded by the survey plane(s), with the exception of sea surface temperature (SST), which was extracted from the 3-day composite SST dataset produced by CSIRO Marine and Atmospheric Research's Remote Sensing Project (see Eveson et al. 2006 for more details).

The environmental conditions during the 2014 survey were close to average in terms of SST and wind speed; however, the level of haze was significantly higher than average (Table 3; Figure 4). Increased haze makes it more difficult to observe surface schools, so we expect the observed sightings rate to be increased in the standardization process (to adjust for the fact that more sightings would likely have been made with less haze).

Table 3. Average environmental conditions during search effort for each aerial survey year.

SURVEY YEAR	WIND SPEED (KNOTS)	SWELL HEIGHT (0-3)	AIR TEMP (°C)	SST (°C)	SEA SHADOW (0-8)	HAZE (0-3)
1993	3.9	0.8	24.4	19.6	1.9	0.9
1994	4.1	1.5	22.7	19.7	2.8	0.5
1995	4.4	1.7	18.7	19.6	2.7	1.1
1996	4.5	1.6	22.9	19.6	2.1	1.2
1997	4.1	1.7	25.3	21.1	1.6	1.3
1998	3.7	1.7	22.3	20.4	0.9	1.7
1999	4.1	0.9	22.0	19.9	2.9	0.7
2000	4.3	0.6	27.5	20.7	2.6	0.7
2005	4.7	1.5	21.7	20.1	1.6	0.8
2006	5.6	1.5	20.0	20.1	3.5	1.0
2007	5.8	1.3	21.6	20.8	2.0	1.3
2008	3.8	1.4	24.2	20.4	1.4	0.9
2009	3.8	1.4	22.3	21.0	2.2	1.7
2010	3.5	1.1	23.6	21.2	1.8	1.2
2011	3.9	1.3	20.2	20.3	2.8	1.4
2012	3.7	1.6	20.7	20.5	4.3	1.8
2013	4.2	1.6	24.6	21.7	2.6	1.6
2014	4.3	1.8	24.0	20.6	2.4	1.9

Figure 4. Boxplots summarizing the environmental conditions present during valid search effort for each aerial survey year. The thick horizontal band through a box indicates the median, the length of a box represents the inter-quartile range, and the vertical lines extend to the minimum and maximum values. The dashed blue line running across each plot shows the average across all survey years.

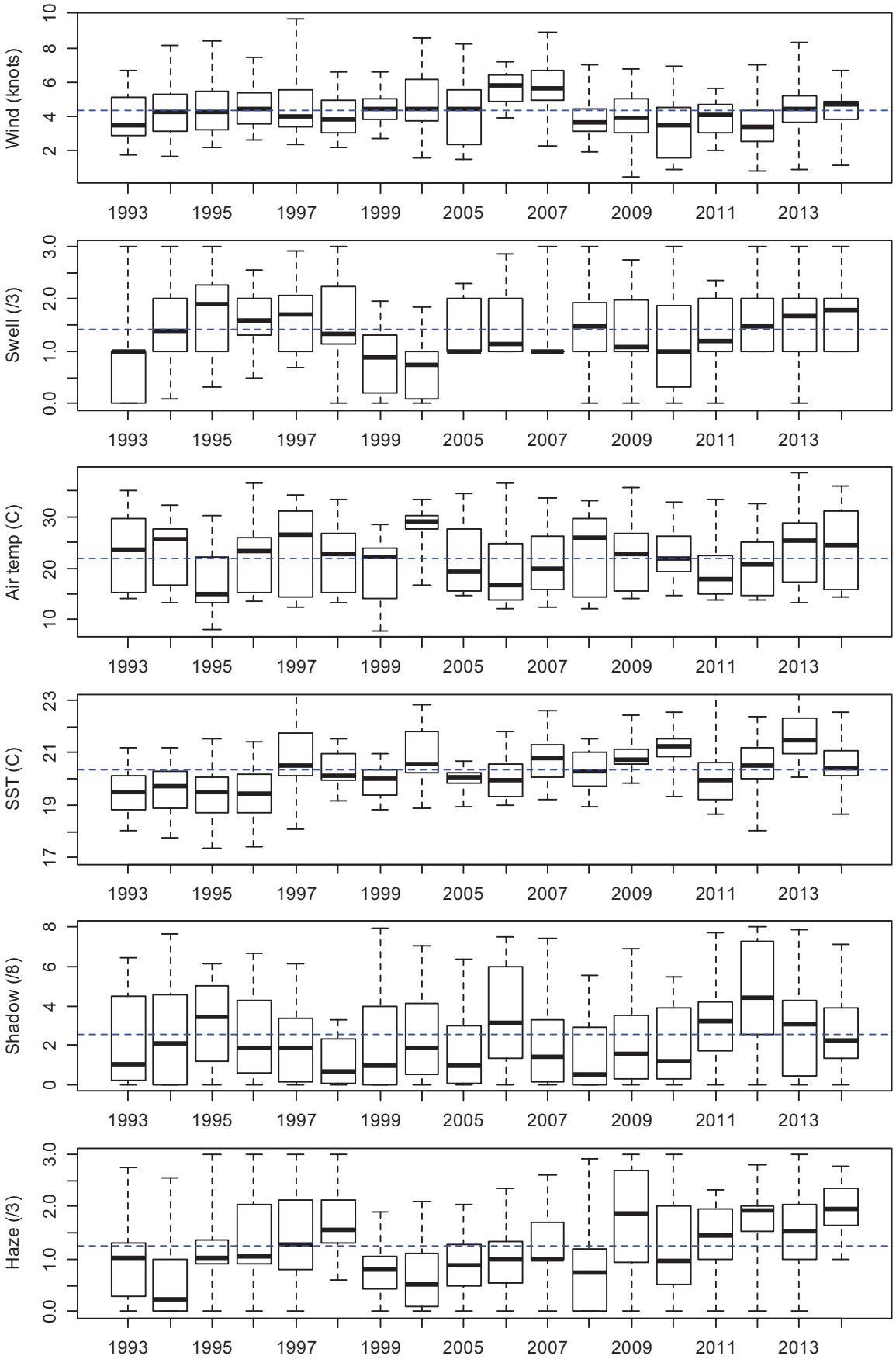

3.5 Method of analysis

The methods of analysis used this year were exactly the same as the past two years. We give a brief description of the methods here, but details can be found in Appendix A.

Generalized linear models were fit to two different components of observed biomass—biomass per sighting (BpS) and sightings per nautical mile of transect line (SpM). We included the same environmental and observer variables in both models as last year (note that sea shadow was added to the SpM model last year). Specifically, the models can be expressed as:

BpS model: logE(Biomass) ~ Year*Month*Area + SST + WindSpeed

SpM model: logE(N_sightings) ~ offset{log(Distance) + log(ObsEffect)} + Year*Month*Area + SST + WindSpeed + Swell + Haze + MoonPhase + SeaShadow

Note that, as of 2011, we include "observer effect" as an offset (i.e., as known) in the SpM model rather than as a linear covariate. The reason for this is discussed in Appendix A of Eveson et al. (2011). Because of this, we need to account for uncertainty in the observer effect estimates through other methods. Such methods have been developed for application to similar problems, but they are computer intensive and we have had difficulties implementing them successfully in this context. Thus, the standard errors, CVs and confidence intervals for the relative abundance indices reported in Table 4 do not include uncertainty in the observer effects for the SpM model (meaning they are slightly too small).

In both models, Year, Month and Area were fit as factors, as was MoonPhase in the SpM model. All other explanatory variables were fit as linear covariates. Note that the term Year*Month*Area encompasses all 1-way, 2-way and 3-way interactions between Year, Month and Area (i.e., it is equivalent to writing Year + Month + Area + Year:Month + Year:Area + Month:Area + Year:Month:Area).

In both models, the 2-way and 3-way interaction terms between Year, Month and Area were fit as random effects, whereas the 1-way effects were fit as fixed effects. Many of the 2-way and 3-way strata have very few (sometimes no) observations, which causes instabilities in the model fits when treated as fixed effects. One main advantage of using random effects is that when little or no data exist for a given level of a term (say for a particular area and month combination of the Area:Month term), we still have information about it because we are assuming it comes from a normal distribution with a certain mean and variance (estimated within the model).

Data from the single-observer flights in 2010 to present can be included in the BpS model without any changes, except that there is only one biomass estimate per school so it is not necessary to take an average over the estimates made by two observers (refer to "Biomass per sighting (BpS) model" section in Appendix A). With regard to the SpM model, we know from the calibration experiments conducted in 2008 and 2009 that a plane with only one observer makes fewer sightings than a plane with two observers. Based on an updated analysis of the calibration experiment data conducted in 2011 (Eveson et al. 2011), we estimate that, on average, a plane with one observer will make about 70% as many sightings as a plane with two observers. We refer to this factor as the "calibration factor". The calibration factor is used to estimate the relative sighting ability (i.e., an "observer effect") for solo observers. Recall that the "observer effect" estimates for the SpM model are calculated based on a pair-wise observer analysis to estimate the relative sighting abilities of all observer pairs that have been involved in past surveys (see Appendix A). In order to estimate a relative sighting ability for a solo observer, we took the average of the relative sighting ability estimates from when this observer flew as part of a pair, and multiplied it by the estimated calibration factor. For example, one of the observers who flew as a solo observer in the 2010 and 2011 surveys has flown as part of two different observer pairs in past surveys, with relative sighting ability estimates of 0.90 and 0.92. If we take the average of these two relative sighting ability estimates and multiply it by the calibration factor of 0.7, this gives a relative sighting ability estimate for this observer when flying solo of 0.64. This gives us "observer effect" estimates for all observer combinations, so we can proceed with fitting the SpM model in the usual way.

Once the models were fitted, the results were used to predict what the number of sightings per mile and the average biomass per sighting in each of the 45 area/month strata in each survey year would have been

under standardized environmental/observer conditions. Using these predicted values, we calculated an abundance estimate for each stratum as 'standardized SpM' multiplied by 'standardized average BpS'. We then took the weighted sum of the stratum-specific abundance estimates over all area/month strata within a year, where each estimate was weighted by the geographical size of the stratum in nm2, to get an overall abundance estimate for that year. Lastly, the annual estimates were divided by their mean to get a time series of relative abundance indices.

We emphasise that it is important to have not only an estimate of the relative abundance index in each year, but also of the uncertainty in the estimates. We used the same process as in the last three years to calculate CVs for the indices, which takes into account uncertainty in the calibration factor estimate. Details can be found in Appendix B. Recall from above that there is still uncertainty in the observer effect estimates for the SpM model which is not currently being accounted for.

We calculated confidence intervals for the indices based on the assumption that the logarithm of the indices follows a normal distribution, with standard errors approximated by the CVs of the untransformed indices.

4 Results

(Results and diagnostics for the BpS and SpM models are provided in Appendix C.)

Figure 5 shows the estimated time series of relative abundance indices with 90% confidence intervals. The point estimates and CVs corresponding to Figure 5 are given in Table 4. Recall from the Methods section that all of the confidence intervals are being slightly underestimated because they do not account for uncertainty in the observer effect estimates.

The 2014 point estimate is the highest of all survey years, and significantly higher when taking confidence intervals into account.

Figure 5. Time series of relative abundance estimates with 90% confidence intervals.

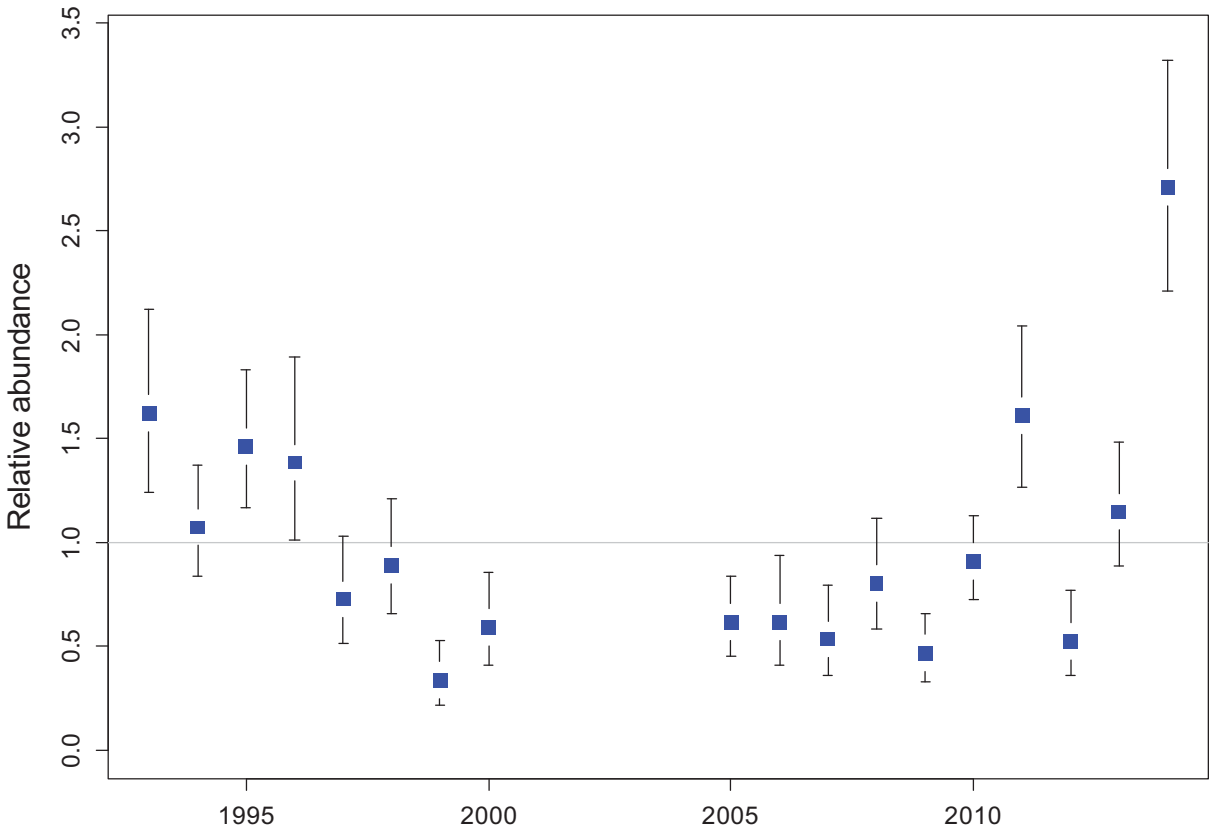

Table 4. Results from the aerial survey analysis.

YEAR	INDEX	SE	CV	CI.05	CI.95
1993	1.62	0.26	0.16	1.24	2.12
1994	1.07	0.16	0.15	0.84	1.37
1995	1.46	0.20	0.14	1.17	1.83
1996	1.38	0.26	0.19	1.01	1.89
1997	0.72	0.15	0.21	0.51	1.03
1998	0.89	0.17	0.19	0.65	1.21
1999	0.34	0.09	0.27	0.21	0.53
2000	0.59	0.13	0.23	0.41	0.86
2005	0.61	0.11	0.19	0.45	0.83
2006	0.62	0.16	0.25	0.41	0.93
2007	0.53	0.13	0.24	0.36	0.79
2008	0.80	0.16	0.20	0.58	1.12
2009	0.46	0.10	0.21	0.33	0.66
2010	0.91	0.12	0.13	0.73	1.13
2011	1.61	0.23	0.15	1.27	2.04
2012	0.52	0.12	0.23	0.36	0.77
2013	1.15	0.18	0.16	0.89	1.48
2014	2.71	0.34	0.12	2.21	3.32

Index = relative abundance point estimates; SE= standard error; CV = coefficient of variation; CI.05 and CI.95 = lower and upper range of 90% confidence interval.

5 Summary

The estimate of relative juvenile abundance from the 2014 scientific aerial survey is significantly higher than for any previous survey year.

The methods of analysis used this year were exactly the same as last two years (Eveson et al. 2012, 2013). Methods to account for uncertainty in the observer effect estimates for the SpM model have yet to be implemented; thus, the CVs for the relative abundance indices do not yet include uncertainty in the observer effects for the SpM model (i.e., they are slightly too small).

The environmental conditions during the 2014 survey were average for the most part, except that the level of haze was higher than usual. Most sightings were made inshore in the eastern half of the survey area. The unusually high percentage of schools comprised of small fish (<8 kg) that were seen in 2009-2013 were not observed this year.

6 References

Anonymous. 2008. Report of the Thirteenth Meeting of the Scientific Committee, Commission for the Conservation of Southern Bluefin Tuna, 5-12 September 2008, Rotorua, New Zealand.

Basson, M., Bravington, M., Eveson, P. and Farley, J. 2005. Southern bluefin tuna recruitment monitoring program 2004-05: Preliminary results of Aerial Survey and Commercial Spotting data. Final Report to DAFF, June 2005.

Bravington, M. 2003. Further considerations on the analysis and design of aerial surveys for juvenile SBT in the Great Australian Bight. RMWS/03/03.

Cowling, A. 2000. Data analysis of the aerial surveys (1993-2000) for juvenile southern bluefin tuna in the Great Australian Bight. RMWS/00/03.

Cowling A., Hobday, A., and Gunn, J. 2002. Development of a fishery independent index of abundance for juvenile southern bluefin tuna and improvement of the index through integration of environmental, archival tag and aerial survey data. FRDC Final Report 96/111 and 99/105.

Eveson, P., Bravington, M. and Farley, J. 2006. The aerial survey index of abundance: updated analysis methods and results. CCSBT-ESC/0609/16.

Eveson, P., Bravington, M. and Farley, J. 2007. Aerial survey: updated index of abundance and preliminary results from calibration experiment. CCSBT-ESC/0709/12.

Eveson, P., Bravington, M. and Farley, J. 2008. The aerial survey index of abundance: updated analysis methods and results. CCSBT-ESC/0809/24.

Eveson, P., Farley, J., and Bravington, M. 2009. The aerial survey index of abundance: updated analysis methods and results. CCSBT-ESC/0909/12.

Eveson, P., Farley, J., and Bravington, M. 2010. The aerial survey index of abundance: updated analysis methods and results for the 2009/10 fishing season. CCSBT-ESC/1009/14.

Eveson, P., Farley, J., and Bravington, M. 2011. The aerial survey index of abundance: updated analysis methods and results for the 2010/11 fishing season. CCSBT-ESC/1107/15.

Eveson, P., Farley, J., and Bravington, M. 2012. The aerial survey index of abundance: updated analysis methods and results for the 2011/12 fishing season. CCSBT-ESC/1208/16.

Eveson, P., Farley, J., and Bravington, M. 2013. The aerial survey index of abundance: updated results for the 2012/13 fishing season. CCSBT-ESC/1309/10.

Appendix A - Methods of analysis

Separate models were constructed to describe two different components of observed biomass: i) biomass per patch sighting (BpS) and ii) sightings per nautical mile of transect line (SpM). Each component was fitted using a generalized linear mixed model (GLMM), as described below. Since environmental conditions affect what proportion of tuna are available at the surface to be seen, as well as how visible those tuna are, and since different observers can vary both in their estimation of school size and in their ability to see tuna patches, the models include 'corrections' for environmental and observer effects in order to produce standardized indices that can be meaningfully compared across years.

For the purposes of analysis, we defined 45 area/month strata: 15 areas (5 longitude blocks and 3 latitude blocks, as shown in Figure A1) and 3 months (Jan, Feb, Mar). The latitudinal divisions were chosen to correspond roughly to depth strata (inshore, mid-shore and shelf-break).

Figure A1. Plot showing the 15 areas (5 longitudinal bands and 3 latitudinal bands) into which the aerial survey is divided for analysis purposes. The green vertical lines show the official transect lines for the surveys conducted in 1999 and onwards; the lines for previous survey years are similar but are slightly more variable in their longitudinal positions and also do not extend quite as far south (which is why the areas defined for analysis, which are common to all survey years, do not extend further south).

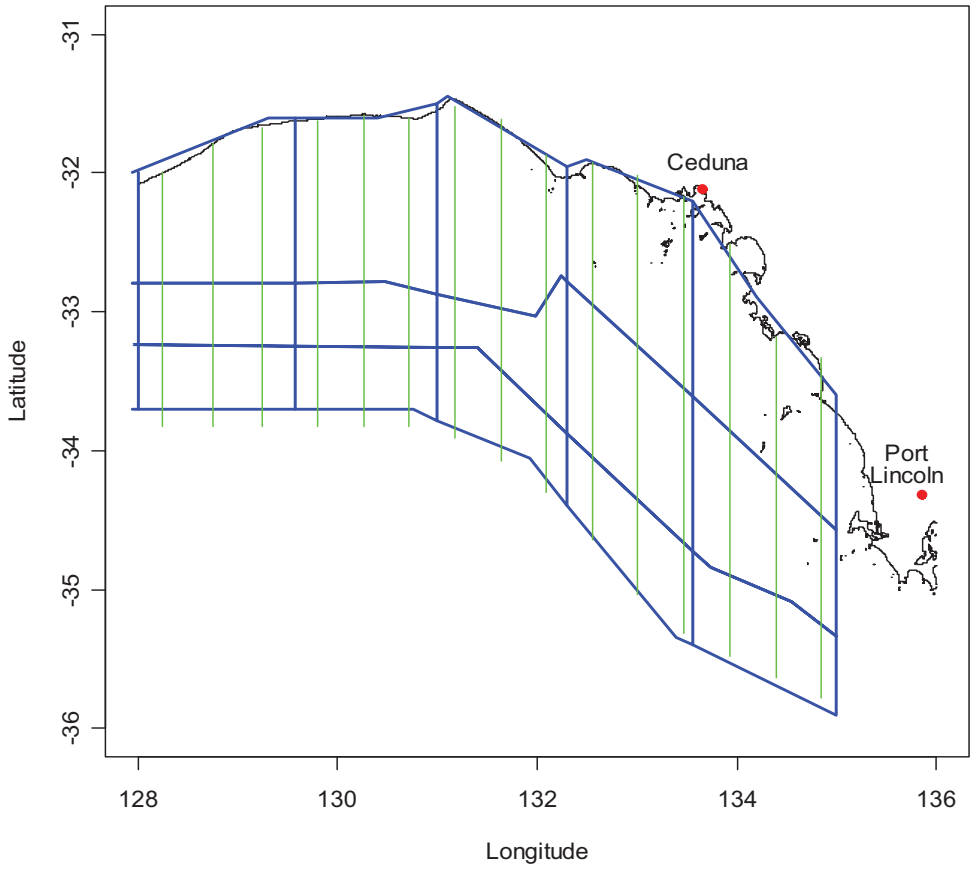

A.1 Biomass per sighting (BpS) model

For the BpS model, we first estimated relative differences between observers in their estimates of patch size (using the same methods as described in Bravington 2003). As in Bravington (2003), we found good consistency between observers. In particular, patch size estimates made by different observers tended to be within about 5% of each other, except for one observer, say X, who tended to underestimate patch sizes

relative to other observers by about 20%. The patch size estimates were corrected using the estimated observer differences (e.g. patch size estimates made by observer X were scaled up by 20%). Because the observer differences were estimated with high precision, we treated the corrected patch size estimates as exact in our subsequent analyses. The final biomass estimate for each patch was calculated as the average of the two corrected estimates (recall that the size of a patch is estimated by both observers in the plane). The final patch size estimates were then aggregated within sightings to give an estimate of the total biomass of each sighting. It is the total biomass per sighting data that are used in the BpS model.

The BpS model was fitted using a GLMM with a log link and a Gamma error structure. We chose to fit a rather rich model with 3-way interaction terms between year, month and area. This is true not only for the BpS model but also for the SpM model described below. In essence, the 3-way interaction model simply corrects the observation (the total biomass of a sighting in the case of the BpS model; the number of sightings in the case of the SpM model) for environmental effects, which are estimated from within-stratum comparisons (i.e. within each combination of year, month and area).

The 2-way and 3-way interaction terms between Year, Month and Area were fit as random effects, whereas the 1-way effects were fit as fixed effects. Many of the 2-way and 3-way strata have very few (sometimes no) observations, which causes instabilities in the model fits when treated as fixed effects. One main advantage of using random effects is that when little or no data exist for a given level of a term (say for a particular area and month combination of the Area:Month term), we still have information about it because we are assuming it comes from a normal distribution with a certain mean and variance (estimated within the model).

Based on exploratory plots and model fits, we confirmed that SST has a significant effect on the biomass per sighting, and that wind speed has a lesser but still significant effect (p-value 0.02; see Appendix C.1). Thus, the final model fitted was

logE(Biomass) ~ Year*Month*Area + SST + WindSpeed

where Year, Month and Area are factors, and SST and WindSpeed are linear covariates (note that E is standard statistical notation for expected value).

A.2 Sightings per mile (SpM) model

For the SpM model, we first ran the pairwise observer analysis described in Bravington (2003), based on within-flight comparisons of sighting rates between the various observers. This analysis gives estimates of the relative sighting efficiencies for the 18 different observer pairs that have flown at some point in the surveys. The observer pairs ranged in their estimated sighting efficiencies from 72% to 97% compared to the pair with the best rate.

We include the (logged) estimates of relative observer pair efficiencies as an offset when fitting the SpM model (i.e., as a predictor variable with a known, rather than estimated, coefficient). Appendix A of Eveson et al. 2011 discusses this in more detail. As such, we need to account for the uncertainty in these estimates through other methods. Such methods have been developed for other applications but have proven difficult to implement in this context. Thus, the standard errors and CVs for the relative abundance indices reported in Table 4 do not include uncertainty in the observer effects for the SpM model (which means they are slightly too small). We will continue to pursue methods of accounting for observer uncertainty in the coming year.

The data used for the SpM model were accumulated by flight and area, so that the data set used in the analysis contains a row for every flight/area combination in which search effort was made (even if no sightings were made). Within each flight/area combination, the number of sightings and the distance flown were summed, whereas the environmental conditions were averaged. The SpM model was fitted using a GLMM with the number of sightings as the response variable, as opposed to the sightings rate. The model

could then be fitted assuming an overdispersed Poisson error structure[3] with a log link and including the distance flown as an offset term to the model (i.e. as a linear predictor with a known coefficient of one).

As we did for the BpS model, we included terms for year, month and area, as well as all possible interactions between them, in the SpM model, and we fitted the 2-way and 3-way interaction terms as random effects (see BpS model section). We determined what environmental variables to include in the model based on exploratory plots and model fits. The final model fitted was:

logE(N_sightings) ~ offset(log(Distance) + log(ObsEffect)) + Year*Month*Area + SST + WindSpeed + Swell + Haze + MoonPhase + SeaShadow

where Year, Month and Area are factors, MoonPhase is a factor (taking on one of four levels from new moon to full moon), and all other terms are linear covariates. Note that MoonPhase is no longer coming out significant (see Appendix C.2) but we chose to keep it in the model for consistency with previous years.

A.3 Combined analysis

The BpS and SpM model results were used to predict what the number of sightings per mile and the average biomass per sighting in each of the 45 area/month strata in each survey year would have been under standardized environmental/observer conditions[4]. Using these predicted values, we calculated an abundance estimate for each stratum as 'standardized SpM' multiplied by 'standardized average BpS'. We then took the weighted sum of the stratum-specific abundance estimates over all area/month strata within a year, where each estimate was weighted by the geographical size of the stratum in nm^2, to get an overall abundance estimate for that year. Lastly, the annual estimates were divided by their mean to get a time series of relative abundance indices.

[3] Note that the standard Poisson distribution has a very strict variance structure in which the variance is equal to the mean, and it would almost certainly underestimate the amount of variance in the sightings data, hence the use of an overdispersed Poisson distribution to describe the error structure.

[4] In our predictions, we used average conditions calculated from all the data.

Appendix B - CV calculations

This appendix provides details of how CVs for the aerial survey abundance indices were calculated.

Let $\hat{B}_{ijk}$ be the predicted value of BpS in year *i*, month *j* and area *k* under standardized environmental/observer conditions (see footnote 4), and $\hat{\sigma}\left(\hat{B}_{ijk}\right)$ be its estimated standard error. Similarly, let $\hat{S}_{ijk}$ be the predicted value of SpM in year *i*, month *j* and area *k* under the same environmental/observer conditions, and $\hat{\sigma}\left(\hat{S}_{ijk}\right)$ be its estimated standard error. Then,

$$\hat{A}_{ijk} = \hat{S}_{ijk}\hat{B}_{ijk}$$

is the stratum-specific abundance estimate for year *i*, month *j* and area *k*.

Since $\hat{B}_{ijk}$ and $\hat{S}_{ijk}$ are independent, the variance of $\hat{A}_{ijk}$ is given by

$$\begin{aligned} V\left(\hat{A}_{ijk}\right) &= V\left(\hat{S}_{ijk}\hat{B}_{ijk}\right) \\ &= V\left(\hat{S}_{ijk}\right)E\left(\hat{B}_{ijk}\right)^2 + V\left(\hat{B}_{ijk}\right)E\left(\hat{S}_{ijk}\right)^2 + V\left(\hat{S}_{ijk}\right)V\left(\hat{B}_{ijk}\right) \\ &\approx \hat{\sigma}^2\left(\hat{S}_{ijk}\right)\hat{B}_{ijk}{}^2 + \hat{\sigma}^2\left(\hat{B}_{ijk}\right)\hat{S}_{ijk}{}^2 + \hat{\sigma}^2\left(\hat{S}_{ijk}\right)\hat{\sigma}^2\left(\hat{B}_{ijk}\right) \end{aligned}$$

The annual abundance estimate for year *i* is given by the weighted sum of all stratum-specific abundance estimates within the year, namely

$$\hat{A}_i = \sum_j \sum_k w_k \hat{A}_{ijk}$$

where w_k is the proportional size of area *k* relative to the entire survey area ($\sum_k w_k = 1$).

If the $\hat{A}_{ijk}$'s are independent, then the variance of $\hat{A}_i$ is given by

$$V\left(\hat{A}_i\right) = \sum_j \sum_k w_k{}^2 V\left(\hat{A}_{ijk}\right)$$

Unfortunately, the $\hat{A}_{ijk}$'s are NOT independent because the estimates of BpS (and likewise, the estimates of SpM) are not independent between different strata. This is because all strata estimates depend on the estimated coefficients of the environmental/observer conditions, so any error in these estimated coefficients will affect all strata. Thus, we refit the BpS and SpM models with the coefficients of the environmental/observer covariates (denote the vector of coefficients by θ[5]) fixed at their estimated values ($\hat{\theta}$). The predictions of BpS and SpM made using the 'fixed environment' models should now be independent between strata, so the stratum-specific abundance estimates calculated using these predictions – which we will denote by $\hat{A}_{ijk}\left(\hat{\theta}\right)$ – should also be independent between strata. Thus, we can

[5] θ contains the environmental/observer coefficients from both the BpS and SpM models; i.e. $\theta = (\theta_{\text{BpS}}, \theta_{\text{SpM}})$

calculate the variance of $\hat{A}_i$ conditional on the estimated values of the environmental/observer coefficients as

$$V\left(\hat{A}_i \mid \hat{\theta}\right) = \sum_j \sum_k w_k{}^2 V\left(\hat{A}_{ijk}\left(\hat{\theta}\right)\right)$$

where $V\left(\hat{A}_{ijk}\left(\hat{\theta}\right)\right)$ is calculated using the formula given above for $V\left(\hat{A}_{ijk}\right)$ but using the BpS and SpM predictions and standard errors obtained from the 'fixed environment' models.

To calculate the unconditional variance of $\hat{A}_i$, we make use of the following equation:

$$\begin{aligned} V\left(\hat{A}_i\right) &= E_\theta\left(V\left(\hat{A}_i \mid \theta\right)\right) + V_\theta\left(E\left(\hat{A}_i \mid \theta\right)\right) \\ &\approx V\left(\hat{A}_i \mid \hat{\theta}\right) + V_\theta\left(\hat{A}_i\right) \end{aligned}$$

where the first term is the conditional variance just discussed and the second term is the additional variance due to uncertainty in the environmental coefficients. The second term can be estimated as follows

$$V_\theta\left(\hat{A}_i\right) \approx \left(\frac{\partial \hat{A}_i}{\partial \theta}\right)' \mathbf{V}_\theta \left(\frac{\partial \hat{A}_i}{\partial \theta}\right)$$

where $\left(\frac{\partial \hat{A}_i}{\partial \theta}\right)$ is the vector of partial derivatives of $\hat{A}_i$ with respect to θ (which we calculated using numerical differentiation), and $\mathbf{V}_\theta$ is the variance-covariance matrix of the environmental coefficients[6].

Now, to account for the additional variance due to uncertainty in the calibration factor, we use a similar approach as above to account for additional variance due to uncertainty in the environmental coefficients. Namely, from the GLM used to estimate the calibration factor, which we will call α, we get an estimate of its variance, which we will call V_α. Then, the variance in the abundance estimates due to uncertainty in α can be estimated by

$$V_\alpha\left(\hat{A}_i\right) = \left(\frac{\partial \hat{A}_i}{\partial \alpha}\right)' V_\alpha \left(\frac{\partial \hat{A}_i}{\partial \alpha}\right)$$

where $\left(\frac{\partial \hat{A}_i}{\partial \alpha}\right)$ is the derivative of $\hat{A}_i$ with respect to α (in essence, it is the amount that the abundance estimate $\hat{A}_i$ changes when the calibration factor is tweaked slightly). Thus, we revise our estimate of $V\left(\hat{A}_i\right)$ by adding on to it $V_\alpha\left(\hat{A}_i\right)$.

---

[6] Recall that θ contains the environmental/observer coefficients from both the BpS and SpM models, so $\mathbf{V}_\theta = \begin{bmatrix} \mathbf{V}_{\theta_{\text{BpS}}} & \mathbf{0} \\ \mathbf{0} & \mathbf{V}_{\theta_{\text{SpM}}} \end{bmatrix}$. The variance-covariance matrices for the individual models are returned from the model-fitting software.

So we have variance estimates for the abundance estimates, but we also want to calculate the variance for the mean-standardized estimates (referred to as the relative abundance indices), calculated as:

$$\hat{I}_i = \frac{\hat{A}_i}{\frac{1}{n}\sum_{i=1}^{n} \hat{A}_i}$$

Using the delta method, we can approximate the variance of $\hat{I}_i$ by

$$V\left(\hat{I}_i\right) \approx \left(\frac{\partial \hat{I}_i}{\partial \hat{A}_i}\right)^2 V\left(\hat{A}_i\right)$$

Then, the standard error of $\hat{I}_i$ is given by

$$\sigma\left(\hat{I}_i\right) = \sqrt{V\left(\hat{I}_i\right)}$$

and the coefficient of variation (CV) of $\hat{I}_i$ is given by

$$\mathrm{CV}\left(\hat{I}_i\right) = \frac{\sigma\left(\hat{I}_i\right)}{\hat{I}_i}.$$

Appendix C - Results and diagnostics

C.1 Biomass per sighting (BpS) model

Figure C1 shows plots of observed biomass per sighting (logged) versus the environmental covariates being included in the BpS model. From these plots, it appears that the size of a sighting tends to increase as SST increases, and possibly decrease as wind speed increases (in a roughly linear fashion in both cases when on a log scale). The relationship with SST appears to be strongest, as supported by the model results (below).

Extract from the output produced by the software used to fit the model (the gam function in the R statistical package mgcv):

```
Family: Gamma
Link function: log

Formula:
Biomass ~ factor(Year) + factor(Month) + factor(Area) + SST + WindSpeed +
Y.M + Y.A + M.A + Y.M.A - 1
```

Parametric Terms:

Covariate	Estimate	SE	t-value	p-
SST	0.116	0.037	3.16	0.002
WindSpeed	-0.053	0.023	-2.33	0.020

```
R-sq.(adj) =  0.0711   Deviance explained = 36.3%
GCV score =  1.964  Scale est. = 1.7348    n = 1984
```

The results support our observations made based on Figure C1; size of a sighting tends to increase as SST increases and decrease as wind speed increases, but that relationship with SST has greater statistical significance.

Figure C2 shows some standard diagnostic plots for generalized linear models, and Figure C3 shows the residuals plotted against a number of factors. These plots do not suggest major problems with the model fit. Ideally there should be no trend in the plots of the square root of the absolute residuals against the fitted values (i.e., lower half of Fig. C2, with left-hand side being on the link scale and the right-hand side being on the response scale); although there is a small kink revealed by a smooth through the data (red line), there is not a consistent increasing or decreasing trend.

Figure C1. Plots of observed biomass per sighting, on a log scale, versus the covariates included in the model; shown is the mean +/- 2 standard deviations.

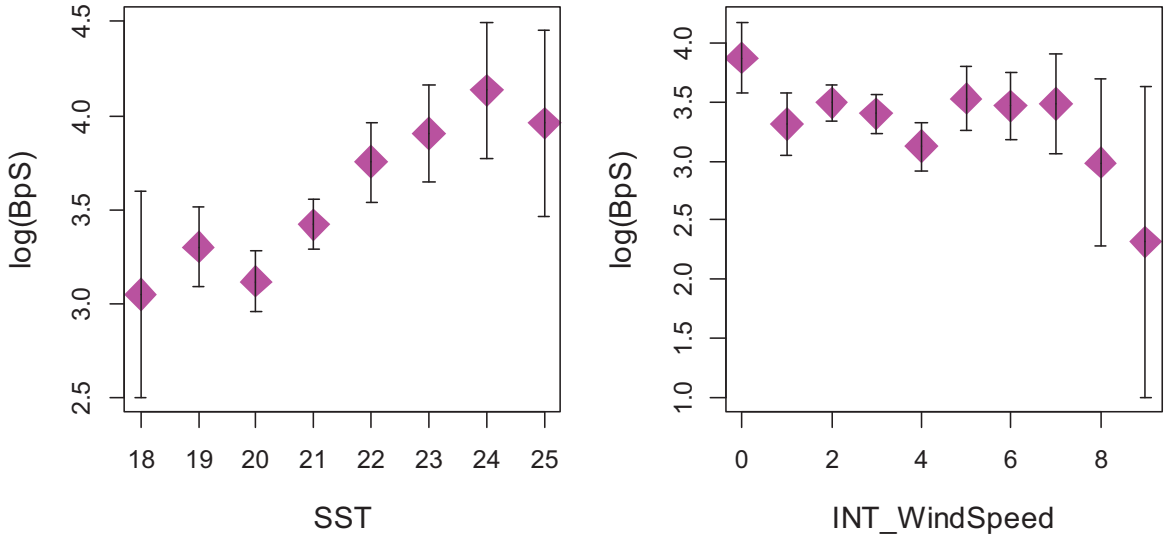

Figure C2. Standard diagnostic plots for biomass per sighting (BpS) model.

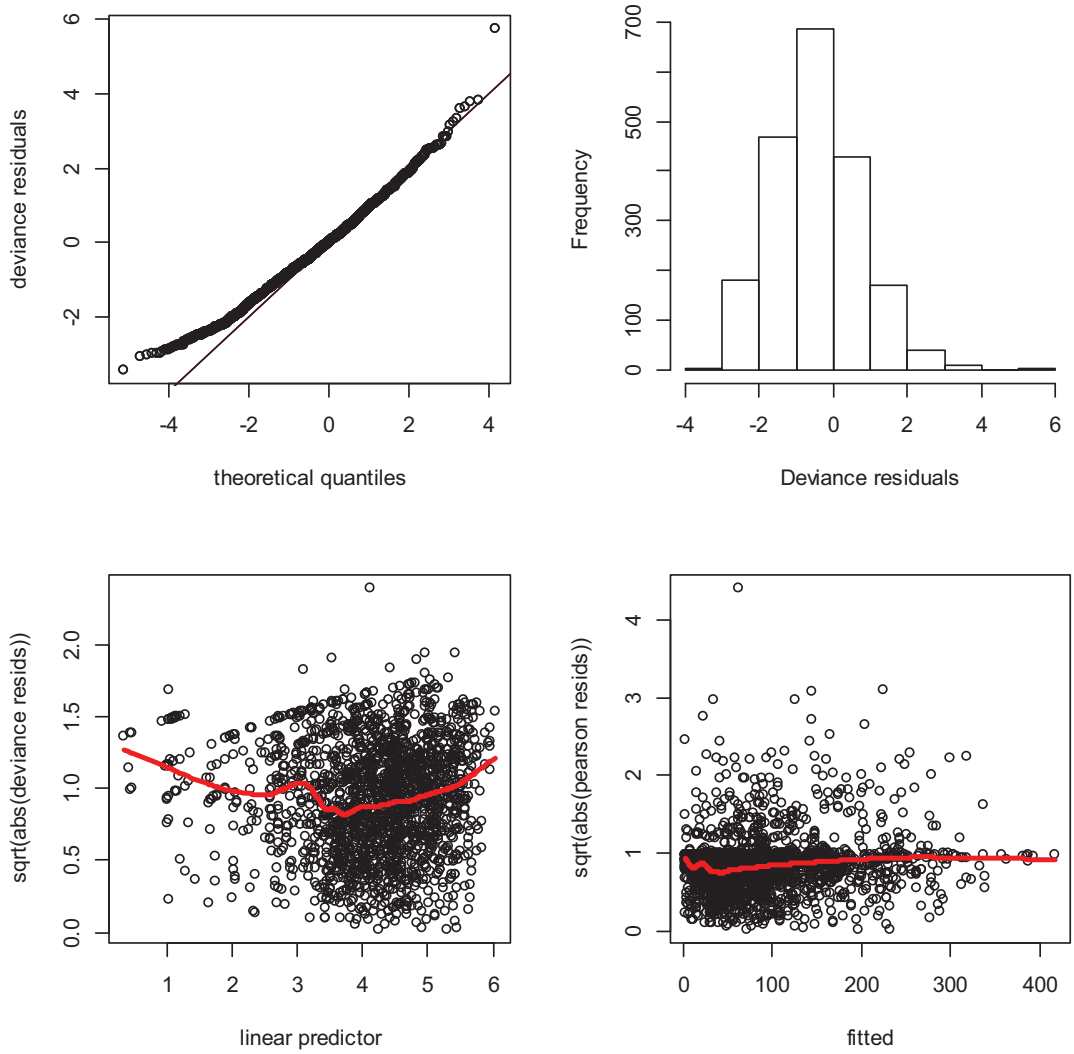

Figure C3. Boxplots of deviance residuals by year, month and area for biomass per sighting (BpS) model.

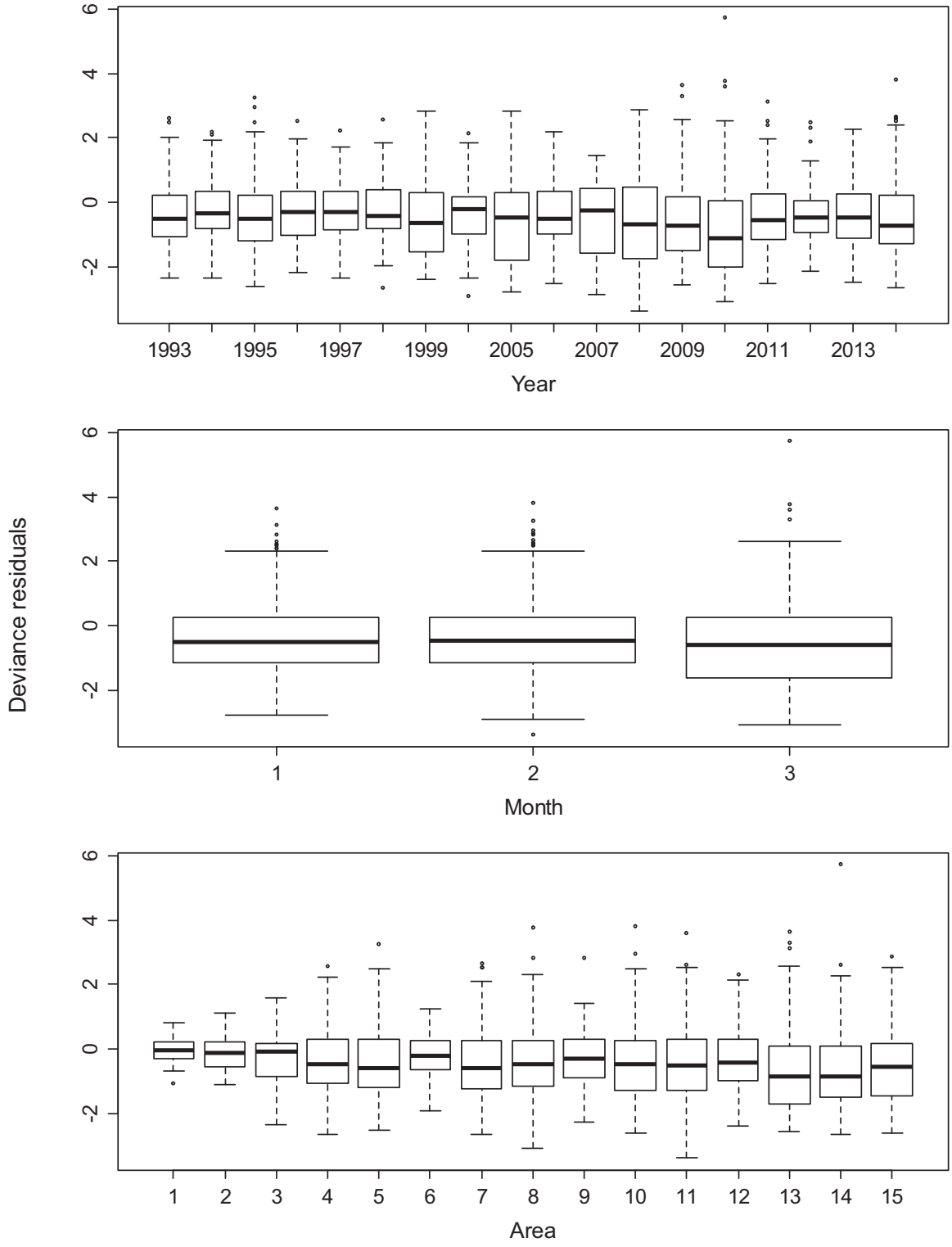

C.2 Sightings per mile (SpM) model

Figure C4 shows plots of observed number of sightings per mile (logged) versus the environmental covariates being included in the SpM model. There appears to be a strong tendency for the rate of sightings to increase as SST increases, and to decline as wind speed, haze, swell and sea shadow increase. With the exception of wind speed, the relationship appears to be linear, and this is even true for wind speed in the range of 1 to 7 knots (where most of the observations occur). Moon phase also appears to influence the sightings rate, with the rate being greatest when the moon phase is 1 (fraction of moon illuminated is 0-25%) or 4 (fraction of moon illumination is 75-100%), but the variance is large so the relationship may not be statistically significant.

Extract from the output produced by the software used to fit the model (the gam function in the R statistical package mgcv):

```
Family: quasipoisson
Link function: log

Formula:
N_sightings ~ offset(log(as.numeric(Distance))) + factor(Year) +
factor(Month) + factor(Area) + Y.M + Y.A + M.A + Y.M.A +
log(ObserverEffect) + AvgWindSpeed + AvgSST + AvgSwell + AvgHaze +
factor(MoonPhase) - 1

Parametric Terms:
```

Covariate	Estimate	SE	t-value	p-value
AvgWindSpeed	-0.271	0.020	-13.38	0.000
AvgSST	0.192	0.032	6.06	0.000
AvgSwell	-0.167	0.049	-3.44	0.001
AvgHaze	-0.159	0.043	-3.66	0.000
AvgSeaShadow	-0.065	0.014	-4.54	0.000
factor(MoonPhase)2	-0.078	0.086	-0.91	0.361
factor(MoonPhase)3	-0.102	0.111	-0.92	0.358
factor(MoonPhase)4	0.072	0.075	0.96	0.336

```
R-sq.(adj) =  0.492   Deviance explained = 66.4%
GCV score = 1.3997  Scale est. = 1.1475    n = 2133
```

The results again suggest that there is a tendency for the rate of sightings to increase as SST increases, and to decline as wind speed, haze, swell and sea shadow increase (all highly significant). The relationship with moon phase is more complex, with the sightings rate being greater when the moon phase is 1 (fraction of moon illuminated is 0-25%) or 4 (fraction of moon illumination is 75-100%), but this relationship is no longer coming out significant at the 0.05 level.

Figure C5 shows some standard diagnostic plots for generalized linear models, and Figure C6 shows the residuals plotted against a number of factors. The Q-Q plot (top left) suggests lack of fit at the tails of the

distribution, which is common; however it also has a strange kink in the centre. Otherwise there are no indications of serious problems with the model fit. The plots of the square root of the absolute residuals against the fitted values (i.e., lower half of Fig. C5, with left-hand side being on the link scale and the right-hand side being on the response scale) look a bit odd, but this is expected because we are modelling count data. A smooth line through these data is reasonably flat, as desired, except for where it follows the residuals for the zero response values (i.e., where the observed number of sightings was zero).

Figure C4. Plots of observed sightings per mile, on a log scale, versus the covariates included in the model; shown is the mean +/- 2 standard deviations.

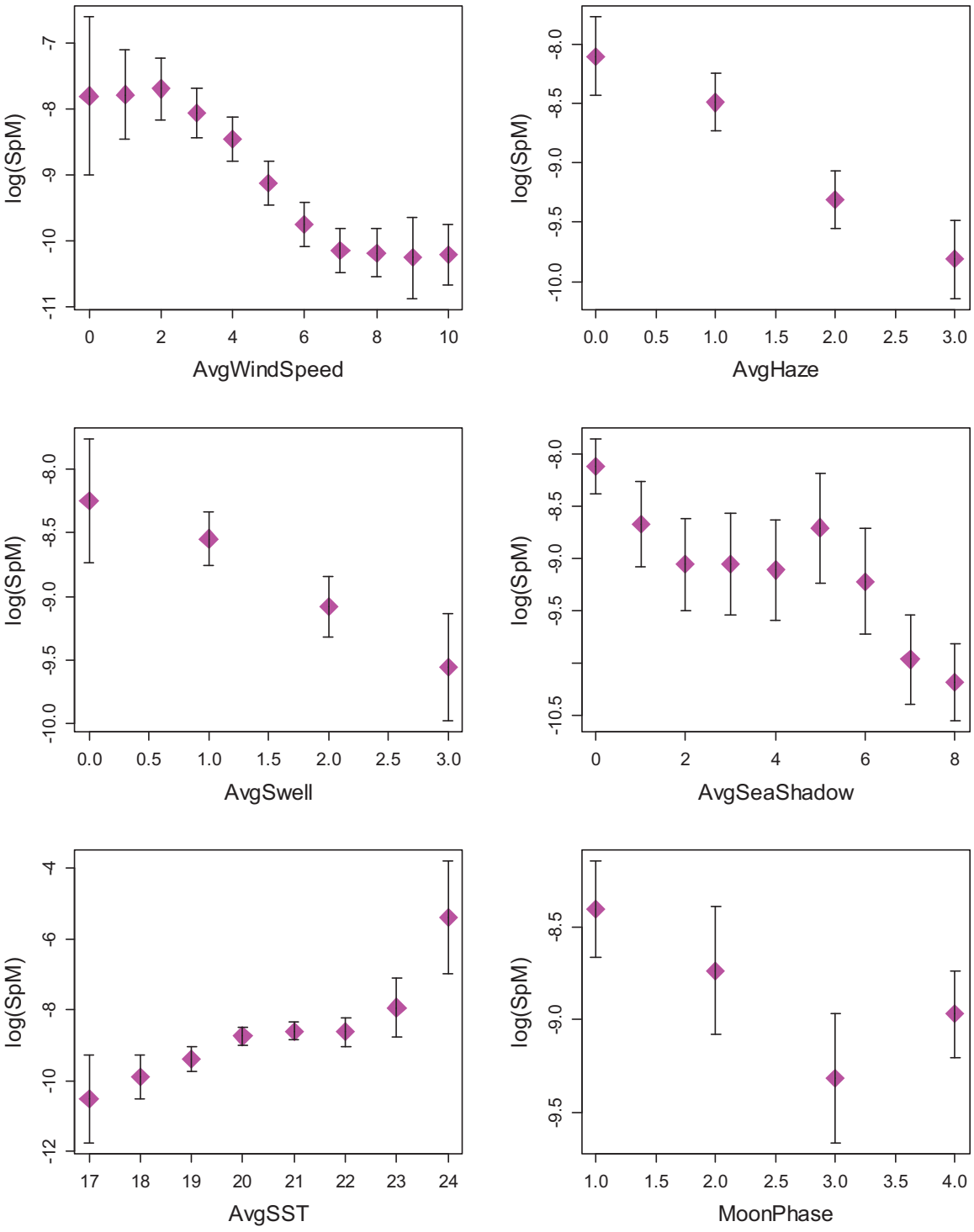

Figure C5. Standard diagnostics plots for sightings per mile (SpM) model.

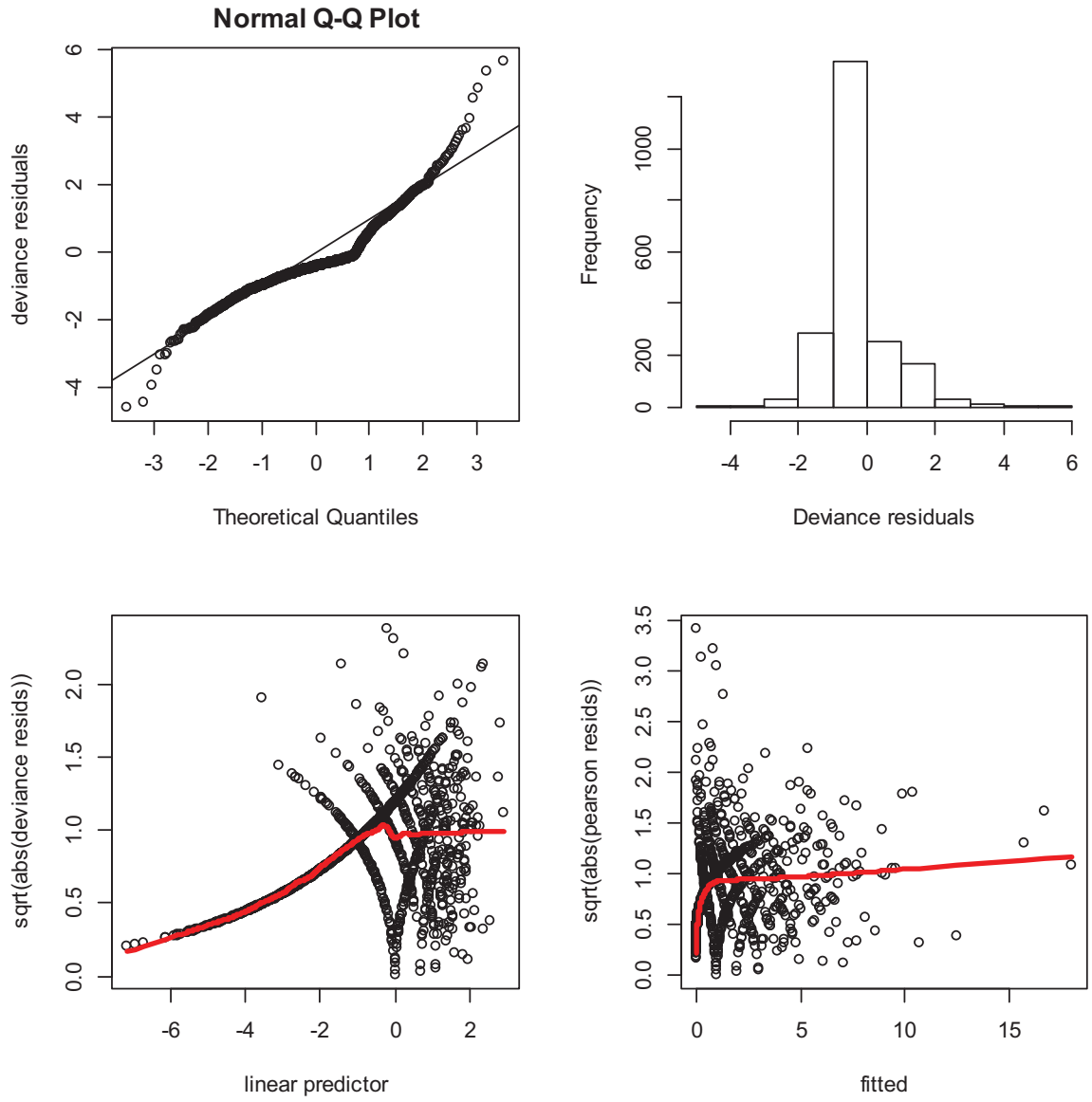

Figure C6. Boxplots of deviance residuals by year, month and area for sightings per mile (SpM) model.

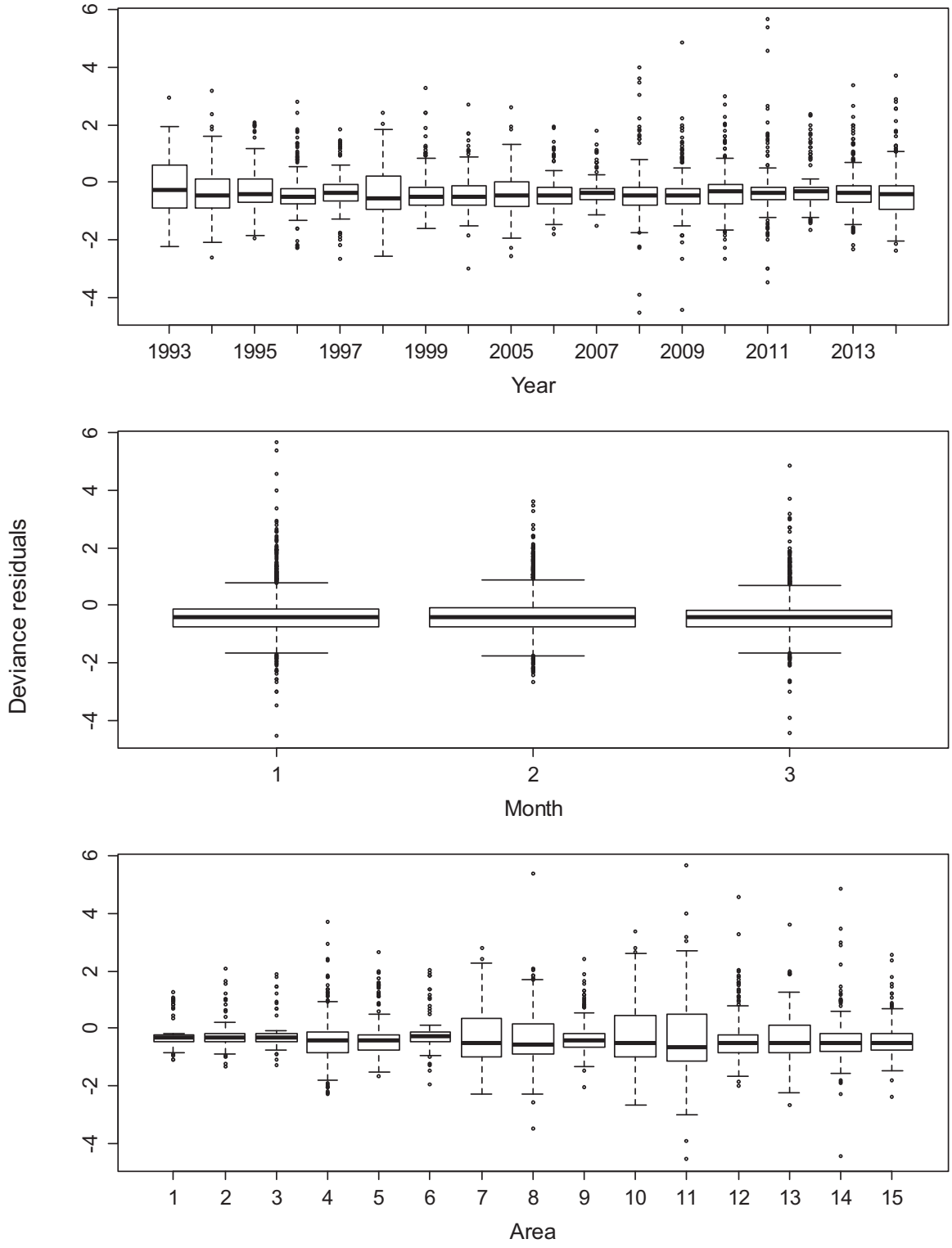

CONTACT US

t 1300 363 400
+61 3 9545 2176
e enquiries@csiro.au
w www.csiro.au

YOUR CSIRO

Australia is founding its future on science and innovation. Its national science agency, CSIRO, is a powerhouse of ideas, technologies and skills for building prosperity, growth, health and sustainability. It serves governments, industries, business and communities across the nation.

FOR FURTHER INFORMATION

CSIRO Oceans and Atmosphere Flagship
Paige Eveson
t +61 3 6232 5015
e paige,eveson@csiro.au
w www.csiro.au